Numerical Simulations of Breaking Waves at vertical wall

F. Gao and J. Zang
Department of Architecture and Civil Engineering, University of Bath
Bath, United Kingdom

ABSTRACT

In this paper, a two-phase flow model is presented for simulating breaking wave impact on a rigid wall. The model is based on the Reynolds-averaged Navier–Stokes equations with the k−ω turbulence model and developed under the framework of the open source CFD library - OpenFOAM. The governing equations are discretized by using the finite volume method and the air-water interface is captured by employing the volume of fluids (VOF) technique. With suitable predefined initial condition, three different types of wave impact on a vertical wall have been generated successfully. Following that, the pressure distribution and velocity field for air pocket impact are analyzed.

KEY WORDS: OpenFOAM; Reynolds-averaged Navier–Stokes (RANS) equations; breaking wave; turbulence.

INTRODUCTION

Over the last few decades, significant advances have been made in the theoretical, experimental and numerical studies of the characteristics of breaking waves. Since small interface deformations, air entrainment and vorticity generation are involved during the overturning and the subsequent impact of the wave, numerical simulation of breaking waves is still a very challenging aim to achieve. Lin and Liu (1999) gave an overview and discussion of the different numerical techniques which have been used for the interface tracking in breaking wave simulation, while Christensen et al. (2002) detailed some advances that have been made in the numerical modelling and the techniques of measurement for the study of the surf zone. However, most of the models are based on single-phase fluid models, in which only the flow in water is considered in the computation, the pressure in the air is taken as a constant, and the boundary conditions are specified at the free surface. During wave breaking, these single-phase fluid models may be inadequate to deal with the air entrainment and splash-up process. Additional complication arises in the treatment of boundary conditions at the highly distorted free surface. Thus, in order to take the air into account for wave breaking, recently, several two-phase flow models, in which both flows in the air and water are solved, have been developed to study the details of breaking waves and the air entrainment during wave breaking (Lubin et al. 2006, Iafrati 2009). Their results shown that two-phase flow model is preferable to study the kinematics and dynamics of water waves during wave breaking.

In present paper, based on the frame of open source CFD tool – OpenFOAM, a new two-phase flow model is developed to simulate the wave propagating, overturning and impacting on vertical wall. With suitable predefined initial condition, three different types of wave impact on a vertical wall have been produced. The results of the pressure distribution and velocity field near the wall for air pocket impact will be presented.

NUMERICAL METHODS

OpenFOAM is a freely available set of applications developed to solve particular problems in continuum mechanics, which consists of a wide range of solvers and libraries. It has gained popularity in coastal engineering studies (Jacobsen et al., 2011). Based on the basic solver of OpenFOAM, a new two-phase flow model is developed for simulating wave breaking. This model is based on the unsteady Reynolds-averaged Navier–Stokes (RANS) equations with the SST k-ω turbulence model. The governing equations are solved by the finite volume method (FVM) for space discretization and implicit Euler scheme for time discretization. A unique methodology PIMPLE algorithm (Jasak, 1996), which is originated by merging Pressure Implicit with Splitting of Operators (PISO) algorithm and Semi-Implicit Method for Pressure-Linked Equations (SIMPLE) algorithm, is utilised for the pressure-velocity coupling and the air-water interface is modelled by the interface capturing method via a high resolution VOF scheme.

Governing Equations

In order to provide an accurate prediction of the wave impact pressure on the wall and the wave run-up value, the Reynolds averaged Navier-Stokes (RANS) equations and continuity equation are employed as the governing equations as follow:

$$\frac{\partial U_i}{\partial x_i} = 0 \tag{1}$$

$$\frac{\partial U_i}{\partial t}+\frac{\partial\left(U_iU_j\right)}{\partial x_j}=-\frac{1}{\rho}\frac{\partial P}{\partial x_i}+\frac{\partial}{\partial x_j}\left[\upsilon\left(\frac{\partial U_i}{\partial x_j}+\frac{\partial U_j}{\partial x_i}\right)\right]+g_i-\frac{\partial\left(\overline{u_i'u_j'}\right)}{\partial x_j} \quad (2)$$

where U_i, P denote the mean velocity and the mean pressure, respectively, u'_i the fluctuating velocity component, ρ the fluid density, v the fluid viscosity, and g_i the gravity acceleration.

SST k-ω Turbulence Model

Since the high Reynolds number is in the problem of breaking wave impacts on the wall, the Menter's Shear Stress Transport (SST) k-ω turbulence model is employed (Menter, 1994):

$$\frac{\partial(\rho k)}{\partial t}+\frac{\partial\left(\rho U_j k\right)}{\partial x_j}=P_k-\beta^*\rho\omega k+\frac{\partial}{\partial x_j}\left[\left(\mu+\sigma_k\mu_t\right)\frac{\partial k}{\partial x_j}\right] \quad (3)$$

$$\frac{\partial(\rho\omega)}{\partial t}+\frac{\partial\left(\rho U_j\omega\right)}{\partial x_j}=\frac{\gamma}{\nu_t}P_k-\beta\rho\omega^2+\frac{\partial}{\partial x_j}\left[\left(\mu+\sigma_k\mu_t\right)\frac{\partial\omega}{\partial x_j}\right]+2\left(1-F_1\right)\frac{\rho\sigma_{\omega2}}{\omega}\frac{\partial k}{\partial x_j}\frac{\partial\omega}{\partial x_j} \quad (4)$$

where P_k is the production rate of turbulence,

$$P_k=\min\left(\tau_{ij}\frac{\partial U_i}{\partial x_j},\,10\beta^*k\omega\right) \quad (5)$$

F_1 is a harmonic function expressed as the following formula,

$$F_1=\tanh\left\{\left\{\min\left[\max\left(\frac{\sqrt{k}}{\beta^*\omega d},\frac{500\nu}{d^2\omega}\right),\frac{4\rho\sigma_{\omega2}k}{CD_{k\omega}d^2}\right]\right\}^4\right\} \quad (6)$$

$$CD_{k\omega}=\max\left(2\rho\sigma_{\omega2}\frac{1}{\omega}\frac{\partial k}{\partial x_j}\frac{\partial\omega}{\partial x_j},\,10^{-10}\right) \quad (7)$$

and $\nu_t=\frac{\mu_t}{\rho}$ is the turbulent kinematic viscosity, μ_t is the turbulent eddy viscosity computed from:

$$\mu_t=\frac{\rho a_1 k}{\max\left(a_1\omega,\Omega F_2\right)} \quad (8)$$

$$F_2=\tanh\left\{\left[\max\left(2\frac{\sqrt{k}}{\beta^*\omega d},\frac{500\nu}{d^2\omega}\right)\right]^2\right\} \quad (9)$$

where d is the distance from the field point to the nearest wall, and Ω is the vorticity magnitude. The constants are:

$\sigma_{k1}=0.85034$, $\sigma_{k2}=1.0$, $\sigma_{\omega1}=0.5$, $\sigma_{\omega2}=0.85616$, $\beta_1=0.075$, $\beta_2=0.0828$, $\beta^*=0.09$, $a_1=0.31$, $\gamma_1=\frac{5}{9}$, $\gamma_2=0.4403$.

Numerical Discretization Schemes

The solution of the Reynolds averaged Navier-Stokes (RANS) and continuity equation is obtained by using PIMPLE, which is merged PISO and SIMPLE algorithms. The implicit Euler scheme is applied for time derivative, and the standard Gaussian finite volume integration is used for discretization in space. The VanLeer scheme is employed for the derivative of convection term. Second order upwind scheme was employed for k and ω. The Vanleer01 scheme is used for the volume fraction α and with α strictly bounded between 0 and 1. Gauss linear scheme is employed for the discretization of gradient term and Laplacian term.

During the procedure of solving the discretized equations, the linear solver PCG (preconditioned conjugate gradient solver) with the preconditioner DIC (diagonal incomplete-Cholesky) is employed for pressure and PBiCG (preconditioned bi-conjugate gradient solver) solver is employed for velocity, k and ω.

NUMERICAL RESULTS AND DISCUSSION

Breaking Wave Generation

From experiments with non-constant slope in front of the wall, Oumeraci et al. (1993) and Bullock et al. (2007) distinguished four types of wave impacts, where the distance between the breaking point and the wall decreases:

Type (a): the aerated impact, where the wave broke in front and hits the wall with an aerated water mass;

Type (b): the air pocket impact, where the wave crest hits the wall with enclosing a thin air bubble;

Type (c): the flip through impact, where the wave crest hits the wall and run up without trapping air bubble;

Type (d): the slosh impact, where the run up of the wave is higher than the wave crest, so that the wave crest hits the water layer instead of the wall.

Generation of breaking waves can be performed by starting from initial deformed free surface, to avoid the whole process simulation from wave-maker up to breaking. With suitable initial free surface shape to do the simulation, the first three types of wave impact on the wall can be easily generated (Scolan et al., 2010). Here we use a hyperbolic tangent shape to define the initial free surface:

$$y=h+A\tanh\left(R\left(x-L/2\right)\right),\quad 0<x<L \quad (10)$$

where L is the length of the wave tank, h is the mean water depth, A is the amplitude of the mode and R is the parameter controls the slope of the difference in height. The shape is defined in a coordinate system where the origin is located at the bottom left corner.

With interested in generating different types of breaking wave, we first test the simulations with three different mean water depth h = 0.19m, 0.24m and 0.32m, the other parameters are kept unchanged as L = 2m, A = 0.16m and R = 5. The height of calculation domain is chosen as 0.6m, which is much higher than the water height of the initial free surface, to leave the space for the air flow and wave impact fully developed. The initial test was curried out with mesh size 300×120 and the time step Δt = 0.005s.

The results of free surface profiles near the wall at different times are shown in Figure 1. It can be seen that three different types of wave impact have been generated relatively with respect to the different mean water depth. For h = 0.19m, an aerated impact is generated, the wave breaking in front of the wall and entrapping an air pocket. When the breaking wave run forward to hit the wall, an aerated water mass will be involved in. For h = 0.24m, an air pocket impact is generated, the wave breaking on the wall with a thin air bubble enclosed between the wave and the wall. For h = 0.32m, a flip through impact is generated, the wave crest hits the wall and run up without trapping air bubble.

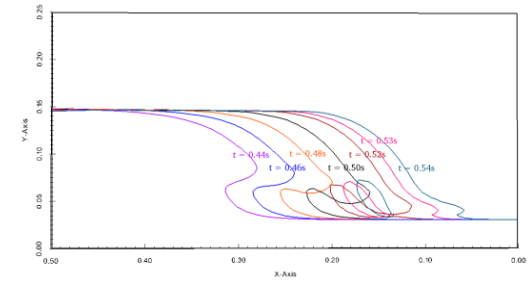

(a) aerated impact (h = 0.19m)

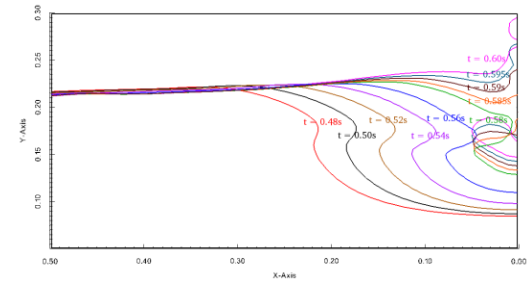

(b) air pocket impact (h = 0.24m)

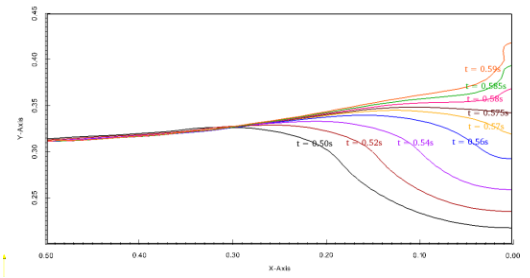

(c) flip through impact (h = 0.32m)

Figure 1. Free surface profiles near the wall at different times

Air Pocket impact simulation

In this paper, we focused on the air pocket impact test. In order to capture the maximum wave impact pressure on the wall, very fine resolution in both space and time is needed. For mesh convergence test, 5 different meshes are tested which are listed in table 1. All of these tests are carried out in the same domain and the same parameter defined initial free surface as before for air pocket impact simulation, the time step $\Delta t = 0.005s$ are kept in same.

Figure 2 shows the time history of free surface elevation at x = 0.5m away from the vertical wall, the results are quite similar. It seems that relatively coarse mesh 1 or 2 is enough to do this simulation. However, as shown in Figure 3 for the time history of pressure at probe located at y = 0.20m on the wall, the fine mesh are needed to catch the maximum impact pressure. Up to the finest mesh 4 and 5, the results are nearly the same, which means the mesh convergence is achieved. In the following simulations, the mesh 4 is used.

Table 1: The mesh size list

Mesh	Nx	Ny
1	300	120
2	600	240
3	900	360
4	1200	480
5	1500	600

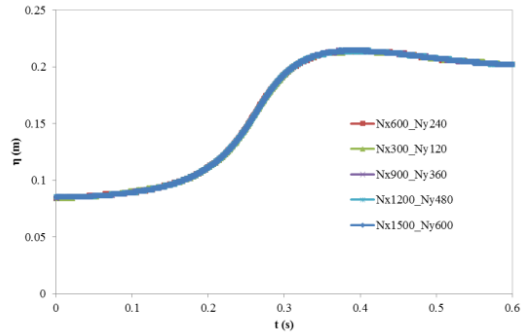

Figure 2. The time history of free surface elevation at x = 0.5m away from the wall.

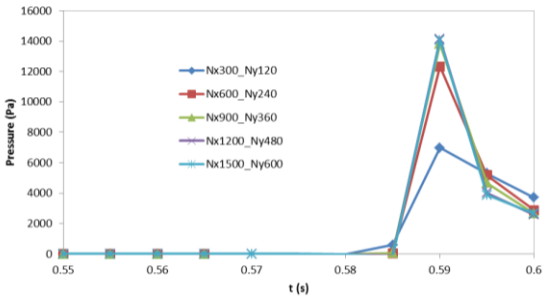

Figure 3. The time history of pressure at probes located y = 0.20m on the wall with different mesh.

With higher frequency of time step used in the simulation, the bigger maximum pressure can be recorded. In this simulation, up to frequency 5000 and 10000, the time history of pressure at the probe located at y = 0.20m on the wall are nearly the same, which can be seen clearly in Figure 4. The following results are obtained by using mesh 4 with frequency 10000.

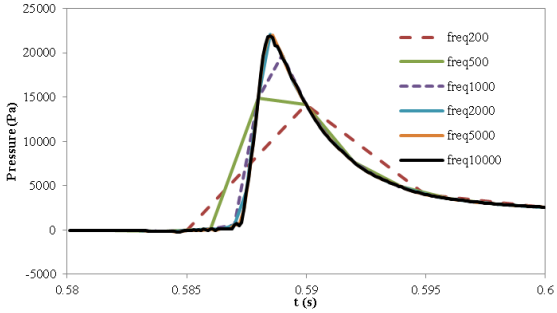

Figure 4. The time history of pressure at probes located y = 0.20m on the wall with different time step.

Figure 5 shows a close view of the pressure distribution and the velocity field during the wave impact on the wall. As the wave crest approaching the wall, the air tends to escape from the entrapment, which leading to a strong air flow in between the wave crest and the wall. The vertical velocity of the air reach its maximum value as the tip of the wave crest hits the wall. At this time, there is a discontinuity of velocity between the water at the tip of the crest and the wall, which lead to a very sharp pressure peak at the contact point. The very sharp and localized impact pressure area can be seen clearly in Figure 5 (c).

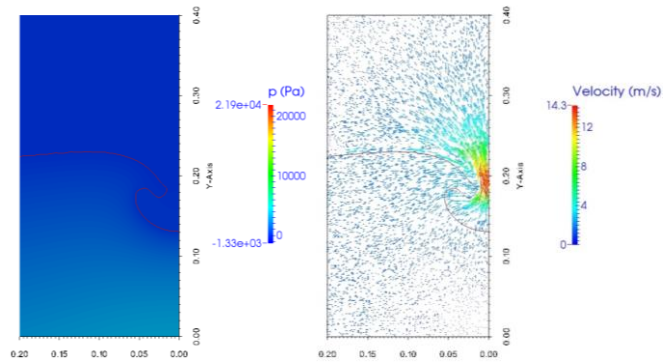

(a) t = 0.580s

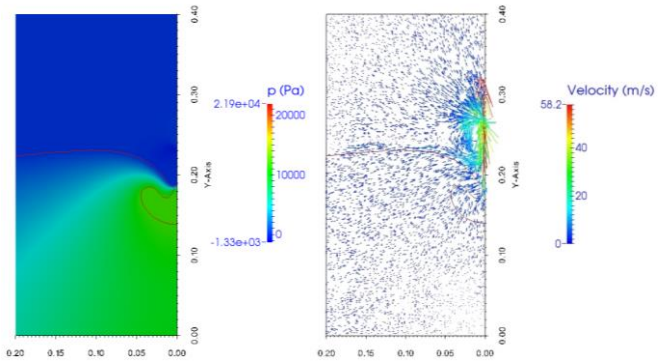

(b) t = 0.585s

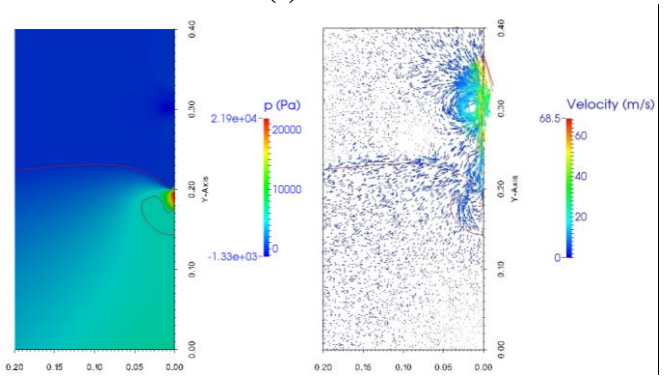

(c) t = 0.588s

Figure 5. Snapshots of the numerical simulations at varioues time. (left is pressure distribution; right is velocity field)

When the wave gets closer to the wall, the water level at the wall is gradually increasing at the points initially below it. This increase in the free-surface level results in a slight increase of pressure in this region. Figure 6 shows the time history of the pressure variations at these points. Inside the air pocket, the pressure is smooth and uniform in time which is the same as observed by other researchers (Costes et al. 2013, Guilcher et al. 2012). The time history of the pressure for probes located inside the air pockets is shown in Figure 7. For the probes located at the impact region, due to the very sharp impact pressure, a very fine resolution in both space and time is required. Figure 8 shows time history of pressure at the probes located around the impact point. It can be seen that the probe located at the y = 0.195m got the peak impact pressure 21949Pa at t = 0.588s. After the wave crest hit the wall, the trapped air pocket will be compressed and the pressure inside it will be oscillated (Lafeber et al. 2012). Unfortunately, the current model is not developed with compressible solver, the pressure oscillating has not been obtained in present simulation.

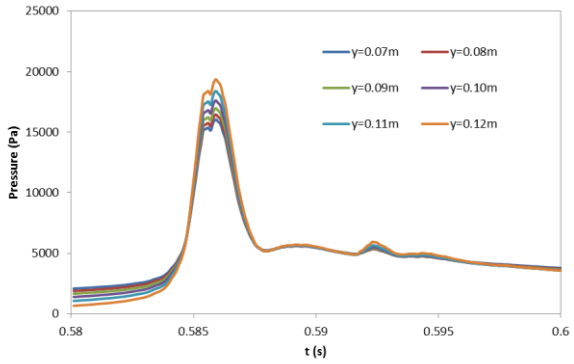

Figure 6. The time history of pressure at probes initially located below the water level on the wall.

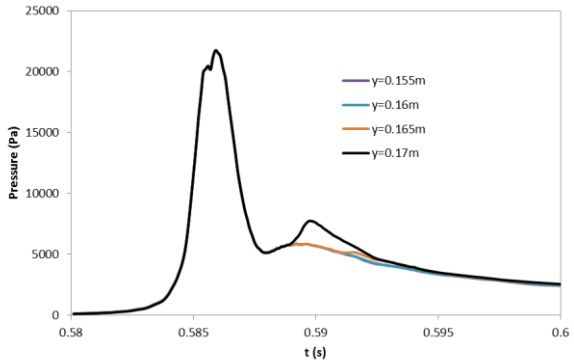

Figure 7. The time history of pressure at probes located inside the air pocket.

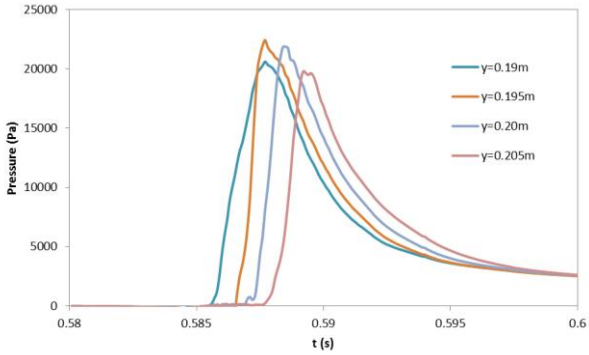

Figure 8. The time history of pressure at probes located around the impact point.

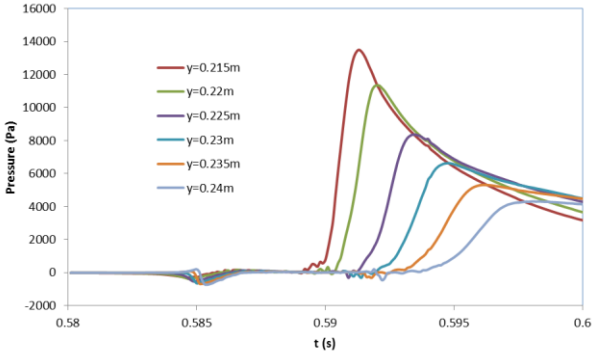

Figure 9. The time history of pressure at probes located above the impact point.

As the wave travels along the wall after the impact, the pressure increases on the probes that get into contact with the run-up and decreases afterwards. This can be seen clearly in Figure 9, the peak value of pressure reduced as the probe location away from the impact point.

CONCLUSIONS

A new two-phase flow model based on OpenFOAM is developed, which is solving the unsteady Reynolds-Averaged Navier-Stokes (RANS) equations couple with k−ω turbulence model. Three types of breaking wave impact on a vertical wall were generated successfully with predefined initial condition. For the air pocket impact, the strong escaping air flow is performed and the high pressure peak at the contact point is captured with fine mesh and small time step. In order to capture the pressure oscillation inside the air pocket, compressible solver is needed to include in the model.

ACKNOWLEDGEMENTS

This research was supported by the United Kingdom EPSRC Project: FROTH (Fundamentals and Reliability of Offshore Structure Hydrodynamics), under grant Ref: EP/J012777/1.

REFERENCES

Bullock, G., Obhrai, C., Peregrine, D., Bredmose, H., 2007. "Violent breaking wave impacts. Part 1: Results from large-scale regular wave tests on vertical and sloping walls". *Coastal Engineering*. Vol 54, pp 602–617

Christensen ED, Walstra DJ and Emarat N (2002). "Vertical variation of the flow across the surf zone", *Coastal Engineering*, Vol 45, pp169-198.

Costes J, Dias F, Ghidaglia JM and Mrabet A (2013). "Simulation of Breaking Wave Impacts on a Flat Rigid Wall by a 2D Parallel Finite Volume Solver with Two Compressible Fluids and an Advanced Free Surface Reconstruction". *Proc 23rd Int Offshore and Polar Eng Conf* (ISOPE), Alaska, USA.

Guilcher PM, Brosset L, Couty N and Le Touz´e D (2012). "Simulations of breaking wave impacts on a rigid wall at two different scales with a two phase fluid compressible SPH model", *Proc 22nd Int Offshore and Polar Eng Conf*. (ISOPE), Rhodes, Greece.

Iafrati A (2009). "Numerical study of the effects of the breaking intensity on wave breaking flows". *Journal of Fluid Mechanics*; Vol 622, pp 371– 411.

Jacobsen NG, Fuhrman DR and Fredsøe J (2012), "A wave generation toolbox for the open-source CFD library: OpenFoam". *International Journal for Numerical Methods in Fluids*, Vol 70, Issue 9, pp 1073–1088.

Jasak H (1996). "Error analysis and estimation for the finite volume method with applications to fluid flows". Ph.D. thesis, Imperial College of Science, Technology and Medicine.

Lafeber W, Brosset L, and Bogaert L(2012). "Elementary Loading Processes (ELP) involved in breaking wave impacts: findings from the Sloshel project". *Proc 22nd Int Offshore and Polar Eng Conf*, (ISOPE), Rhodes, Greece.

Lin, P and Liu, PL-F (1999). "Free surface tracking methods and their applications to wave hydrodynamics", Vol. 5 of *Advances in Coastal and Ocean Engineering*, World Scientific, pp 213-240.

Lubin P, Vincent S, Abadie S, Caltagirone JP (2006). "Three-dimensional large eddy simulation of air entrainment under plunging breaking waves". *Coastal Engineering*; Vol 53, no 8, pp 631–655.

Menter FR (1994), "Two-Equation Eddy-Viscosity Turbulence Models for Engineering Applications", *AIAA Journal*, Vol. 32, no 8, pp 1598-1605.

Oumeraci H, Klammer P and Partenscky HW (1993). "Classification of breaking wave loads on vertical structures". *Journal of Waterway, Port, Coastal, and Ocean Engineering.* Vol 119, no 4, pp 381–397.

Scolan Y-M (2010), "Some aspects of the flip-through phenomenon: A numerical study based on the desingularized technique," *Journal of Fluids and Structures*, Vol 26, Issue 6, pp 918-95.